miR-124-3p and miR-181a-5p Mediate AT1-Receptor Autoantibody Induced Fetal Rat Cardiac Remodeling via Increased VCAN Expression

Mingming Yue
Capital Medical University
Yan Sun
Yang Li
Pengli Wang
Chunyu He
Lina Bai
Ye Wu
Shuhai Lan
Wayne Lau
Xin-Liang Ma
Thomas Jefferson University
Suli Zhang
Huirong Liu (liuhr2000@ccmu.edu.cn)
Capital Medical University

Article

Keywords: Autoantibody against angiotensin II type 1 receptor, miR-124-3p, miR-181a-5p, cardiac remodeling, VCAN

Posted Date: March 11th, 2022

DOI: https://doi.org/10.21203/rs.3.rs-1430465/v1

Abstract

Autoantibodies against angiotensin II type 1 receptor (AT1-AA) are prevalent in preeclampsia. They induce fetal cardiac structural remodeling in late pregnancy via still unknown mechanisms, the subject of this study's investigation. MicroRNA array revealed differential expression of microRNAs in fetal hearts exposed to AT1-AA. miR-124-3p and miR-181a-5p, the most significantly altered microRNAs, were significantly enriched in the myocardium. Gain- and loss-of-function experiments demonstrated that miR-124-3p and miR-181a-5p governed cardiomyocyte phenotype. Overexpression of miR-124-3p or inhibition of miR-181a-5p activated neonatal rat cardiomyocyte proliferation and size (the converse also being true). Moreover, miR-124-3p overexpression and miR-181a-5p inhibition acted in concert to exacerbate the effects of AT1-AA (increasing the size and proliferation of neonatal rat cardiomyocytes). Through TMT™ quantitative proteomics and luciferase reporter gene assay, miR-181a-5p and miR-124-3p respectively target the 3' UTR and 5'UTR of VCAN, and oppositely regulate its expression. VCAN knockdown in neonatal rat cardiomyocytes blocked the pathological effect of AT1-AA. Furthermore, ELISA demonstrated positive correlation between AT1-AA expression and VCAN level in preeclamptic patient umbilical cord blood. Our study demonstrates that upregulation of miR-124-3p promotes VCAN expression, and miR-181a-5p downregulation decreases VCAN inhibition, thereby co-mediating AT1-AA induced fetal cardiac remodeling.

Introduction

During pregnancy, the intrauterine environment is intimately influential upon fetal development, with even slight maternal changes impacting fetal developmental progress[1,2]. The heart is the first developmentally functional organ in mammals. If the fetus encounters an adverse intrauterine environment, its cardiac structure undergoes adaptive changes to ensure maximal operational efficiency, thereby considered cardiac remodeling. Cardiac remodeling during the fetal period persists into postnatal life, and increases adulthood CVD risk[3].

Preeclampsia (PE), causative of an adverse intrauterine environment, threatens fetal health[4,5]. PE patient fetuses manifest cardiac swelling, decreased left ventricular function, and elevated umbilical cord blood BNP levels[6–9]. The mechanisms underlying altered intrauterine cardiac development in the setting of PE are not fully understood. During PE, abnormal activation of the renin-angiotensin system (RAS) has garnered primary focus. In normal pregnancy, the sensitivity of angiotensin II type 1 receptor (AT1R) to angiotensin II (Ang II) decreases. In PE, AT1R is overactivated despite decreased levels of Ang II[10], suggesting the involvement of other factors in excess AT1R activation. In the late 1990s, researchers discovered that 70% of PE patients harbored a class of autoantibody against AT1R (AT1-AA)[11]. In contrast to angiotensin II (which classically transiently activates AT1R), AT1-AA constantly activates AT1R by binding to the extracellular second loop of AT1R (AT1R-ECII)[12]. Intravenous injection of AT1-AA results in PE-like symptoms in mice (eg elevated blood pressure and proteinuria[13–15]). Our previous studies demonstrate the ability of AT1-AA to cross the placental barrier and enter offspring via

lactation[16]. AT1-AA exposure disrupted cardiac structure and function in early life (gestation day 18) [17], but via unclear mechanisms.

MicroRNA (miRNA), a class of endogenous non-coding RNA, post-transcriptionally regulates target gene expression[18]. miRNAs participate in different stages of heart development, as well as cardiac remodeling and regeneration. miRNAs are also a novel therapeutic target[19]. It remains unknown which miRNAs are involved in fetal rat cardiac remodeling induced by AT1-AA. As miRNAs critically regulate cardiac development and cardiovascular diseases, we hypothesize that AT1-AA exposure in utero induced fetal cardiac remodeling by altering the expression of specific miRNAs. This study screened differentially expressed miRNAs, and demonstrated the potential involvement of two key miRNAs during AT1-AA exposure-induced fetal rat cardiac remodeling.

Materials And Methods

Patients and samples

This study complied with the Declaration of Helsinki and was approved by the Ethical Review Committee of Tianjin Baodi Hospital. Informed consent was obtained from all patients (ethical number: TJBDLL20210013). The current study enrolled patients (2020-2021) diagnosed with preeclampsia per clinical diagnostic criteria[20] and normal pregnant women. Detailed baseline patient characteristics are listed in Table S1.

Preparation of AT1-AA

As mentioned in our previous study[21], the functional second loop epitope peptide of human AT1R (165-191: IHRNVFFIINTNITVCAFHYESQNSTL, AT1R-ECII) was hypodermically injected into male AT1-AA negative Sprague-Dawley rats. 8 weeks after injection, serum was collected. AT1-AA was purified from serum by Hi Trap™ Protein G Kit (GE Healthcare, 17-0404-01). AT1-AA concentration and purity were measured by Bicinchoninic Acid Assay (Thermo Scientific™, 23225) and SDS-PAGE respectively.

Animal experiments

All animal experiments were approved by the Institutional Animal Care and Use Committee and Ethics Committee of Capital Medical University. The model of AT1-AA-positive pregnant rats was established by a passive immunization method as previously described[22]. Female Sprague-Dawley rats were mated with male rats overnight. Presence of a vaginal plug the next morning was indicative of embryonic day 0.5. Pregnant rats were divided into control (receiving saline) and treatment (receiving AT1-AA) groups. On gestation day 13 and 15, pregnant rats were injected with AT1-AA (20 μg/g) and saline (identical volume) respectively. Blood pressure was determined (standard tail-cuff method) of pregnant rats on gestation day 12, 14, 16, and 18, followed by tail vein sampling to determine AT1-AA titer. On gestation day 18, after anesthetization by intraperitoneal sodium pentobarbital (150 mg/kg), pregnant rats

underwent laparatomy, and fetal hearts were collected for further analyses. All rats were housed at room temperature (25°C), under a 12 hour light/12 hour dark cycle.

Histological analysis

H&E staining distinguished cardiac morphological changes, and WGA staining aided cardiomyocyte cross-sectional area determination. For H&E staining, fetal heart samples collected on gestation day 18 were fixed with 4% paraformaldehyde, embedded in paraffin, cut into 4-μm-thick sections, and stained per protocol. For WGA staining, the heart paraffin sections were stained with wheat germ agglutinin coupled to Alexa Fluor 488 (Invitrogen, W11261, dilution of 1:100 for 1 hour) and visualized with a laser scanning confocal microscope.

Microarray analysis

The differential expression of microRNAs between control and AT1-AA group was detected by MiRCURY™ LNA expression array (KangChen Bio-tech). Briefly, total fetal heart RNAs from treatment groups were extracted by TRIzol (Invitgen) and microRNAsy mini Kit (QIAGEN) per manufacturer protocol. After RNA measurement using NanoDrop1000, the samples were labeled with miRCURY™ Hy3™/Hy5™ Power Labeling kit and hybridized on the miRCURY™ quantity LNA array. After the washing step, slides were analyzed by Axon GenePix 4000B microarray scanner. Scanned images were imported into GenePix Pro 6.0 software (Axon) for grid alignment and data extraction. The average value of replicated microRNAs was determined, with the normalization factor calculated by selecting the microRNAs with intensity>30 in all samples. Data was subjected to Median normalization, and differentially expressed microRNAs were identified by volcano map screening. Finally, hierarchical clustering was performed to exhibit distinguishable microRNA expression profiles between the treatment groups.

Western blot analysis

Protein samples from heart tissues and NRCMs were lysed with RIPA buffer and PMSF. Concentrations of different samples were evaluated by BCA Protein Assay Kit (Thermo Scientific, Waltham, MA). Equal amounts of total protein (20-50 μg per lane) were separated on ~6-15% SDS-PAGE gels, and electrotransferred onto polyvinylidene fluoride (PVDF) membranes (Millipore, Billerica, MA). The membranes were blocked with 5% milk in TBST for 1 hour at room temperature and incubated with corresponding primary antibodies at 4°C overnight. The employed antibodies were as follows: anti-ANP (ab225844, Abcam), anti-BNP (orb382908, Biorbyt), anti-β-MHC (ab50967, Abcam), anti-PCNA (10205-2-AP, Proteintech), and anti-VCAN (ab177480, Abcam). The next day, after TBST washing, the membranes were incubated with HRP-conjugated secondary antibodies at a 1:1000-5000 dilution range for 1 hour at room temperature, and developed using ECL reagent (Applygen Technologies Inc.). All experiments were performed in triplicate.

Primary neonatal rat cardiomyocytes culture

Cardiomyocytes were isolated from neonatal Sprague-Dawley rats (1-3 days old) using trypsin (without EDTA) and collagenase type II (Gibco). Briefly, cut the skin of the chest and squeeze the back of the neonatal rat firmly to expose the heart. Hearts were excised and placed in precooled PBS, after rinsing 3–4x. Each ventricle was collected and cut into 1-mm^3 tissue blocks. The tissue blocks were then digested repeatedly (approximately 10 times) for ~6 minutes in a 1:2 mixture of trypsin (without EDTA) and collagenase type II (Gibco). The suspension (including cells and enzyme) was gently mixed and added to high-glucose Dulbecco's Modified Eagle's Medium (DMEM) containing 10% fetal bovine serum (FBS) and a 1% mixture of penicillin and streptomycin to terminate the digestion. After filtration, centrifugation (1000 rpm, 10 minutes, RT), and resuspension, cells were plated on a 10-cm^2 petri dish for 1.5-2 hours for cardiac fibroblast removal. Finally, the cardiomyocytes were seeded into 6-well plates or 60-cm^2 petri dishes for further experiments.

Fluorescence in situ hybridization

MicroRNA fluorescence in situ hybridization (FISH) was performed via RNA FISH kit (Genepharma, Shanghai). Briefly, NRCMs were fixed with 4% paraformaldehyde for 15 minutes at room temperature. After fixation, the cells were permeabilized with 0.1% Triton X-100 for 15 minutes at room temperature and washed with PBS. Cells were then incubated with 2x SSC at 37℃ for 30 minutes. After incubation, the hybridization was measured using hybridization buffer with fluorescence-labeled probes via overnight incubation in a 37℃ water bath. The next morning, after discarding the hybridization buffer, the cell slides were washed with 42℃ preheated 1% Tween 20 for 5 minutes, and washed sequentially with 42℃ preheated 2xSSC and 1xSSC. Finally, the cell slides were washed with PBS and stained with mounting medium containing DAPI. Relative FISH probe sequences are displayed in Supplemental Table 3.

Immunofluorescence staining

NRCMs were fixed in 4% paraformaldehyde for 10 minutes at room temperature and washed with PBS. Cells were immersed in 0.5% Triton X-100 3 times (10 minutes each). Goat serum (10%) was applied to the cells for blocking for 30 minutes at room temperature. The cells were incubated with primary antibodies at 4℃ overnight. Employed antibodies were as follows: anti-ki67 (AF0198, Affinity Biosciences), anti-α-actin (23660-1-AP, Proteintech), and anti-VCAN (bs-2533R, Bioss). The next day, after PBS washing, the cells were incubated with fluorescein-conjugated secondary antibodies for 1 hour. After incubation, the cells were washed with 0.5% Triton X-100 and PBS, stained with DAPI, and finally visualized via laser scanning confocal microscopy.

Dual luciferase reporter gene assay

For the luciferase assays, HEK293 cells were transfected with miR-124-3p mimics, miR-181a-5p mimics, and a negative control combined with the corresponding luciferase reporter plasmid of pischeck2-VCAN 5'UTR or psicheck2-VCAN 3'UTR. After co-transfection, the cells were harvested to measure the luciferase activity using a dual luciferase assay kit per manufacturer protocol (DL101-01, Vazyme). The specific

target activity was expressed as the relative activity ratio of firefly to renilla luciferase. At least 3 independent transfections were performed for each experimental group.

Isolation of microRNA and PCR

MicroRNAs were extracted from heart tissues and neonatal rat cardiomyocytes via miRNeasy Mini Kit (OMEGA, R6842-01) per manufacturer instructions. After microRNA extraction, reverse transcription and qPCR were measured with a microRNA Detection Kit (GenePharma, Shanghai, China). qPCR was completed using an ABI 7500 Fast Real Time PCR system (Life Technologies). Relative amounts of transcripts were normalized to the internal control U6 and calculated by the $2^{-\Delta\Delta Ct}$ formula. Primer sequences for real time qPCR are displayed in Supplemental Table 2.

Transfection of shRNA adenovirus, microRNAs, and plasmid

shRNA adenovirus targeting rat VCAN was designed and synthesized by Vigenebio (Shandong, China), and the corresponding control was also purchased from Vigenebio. For microRNA, the miR-124-3p and miR-181a-5p mimic, inhibitor, and negative control RNAs were designed and synthesized by Genepharma (Shanghai, China). For plasmid, sequences of the VCAN gene 3'UTR containing miR-181a-5p target sites and the 5'UTR containing miR-124-3p target sites were inserted into the psicheck2 dual luciferase microRNA target expression vector. Transfection was performed with Lipofectamine 2000 per manufacturer instructions. After 4-6 hours of transfection, NRCMs treated with or without AT1-AA were harvested and lysed for Western blot analysis, while HEK 293A cells were used for the dual luciferase reporter assays.

Enzyme-Linked ImmunosorbentAssays (ELISA)

For AT1-AA titer testing, a biotin-avidin enzyme-linked immunosorbent assay (BA-ELISA) was performed as previously described[22]. Peptides corresponding to the sequence of the second extracellular loop of human AT1R were synthesized at 98% purity. The results were expressed as optical density (OD) and measured at 405 nm via ELISA plate reader (SpectraMax Plus; Molecular Devices, Sunnyvale, CA, USA). For VCAN testing, ELISA was performed per manufacturer instructions (Cloud Clone Corp., SEB817Hu; Cusabio, CSB-EL025810RA).

TMT-labeled quantitative proteomics

Total sample (saline and AT1-AA groups) protein was extracted. A portion of the protein was removed to determine the concentration for SDS-PAGE, while another portion was subjected to trypsin hydrolysis and labeling. The labeled samples underwent chromatographic separation; LC-MS/MS analysis screened credible and differentially expressed proteins. Experimental data was analyzed by Proteome Discoverer TM 2.2 (Thermo) software. The UniProt rat database was used. The false positive rate of peptide identification was controlled <1%.

Bioinformatic analysis

Heatmaps of microRNA array and proteomics were plotted at http://www.bioinformatics.com.cn, a free online platform for data analysis and visualization.

Statistical analysis

All data were expressed as mean±SEM. The Student's t-test analyzed the differences between two groups. One-way ANOVA compared the differences between multiple groups. $P<0.05$ was considered statistically significant. Drafting and statistical analysis was performed using GraphPad Prism 8.0 software (GraphPad Software, Inc., San Diego, CA, USA).

Results

Exposure to AT1-AA resulted in fetal cardiac remodeling.

AT1-AA was purified per previously described protocol (Supplemental Figure 1A)[23]. The biological activity of AT1-AA was verified by increased neonatal rat cardiomyocyte beat rate (Supplemental Figure 1B). After injection of AT1-AA at gestation day 13 and 15, systolic blood pressure (SBP) and the AT1-AA P/N value were significantly increased, indicating successful establishment of the AT1-AA-positive pregnant rat model (Supplemental Figures 2A, B). Fetuses from the AT1-AA group exhibited greater heart/body weight ratio (HW/BW) (Figure 1A, Supplemental Figure 3), thicker left ventricular wall (Figure 1B), increased cardiomyocytes cross-sectional area (Figure 1C), and greater ki67-positive cardiomyocyte proportion (Figure 1D) since gestation day 18. Increased expression of fetal genes such as ANP, BNP, β-MHC, and the proliferation marker PCNA (Figure 1E) suggested AT1-AA exposure in utero caused cardiomyocyte proliferation through late pregnancy. *In vitro*, the direct effect of AT1-AA was observed in isolated primary neonatal rat cardiomyocytes (NRCMs). Under AT1-AA stimulation, the proportion of ki67-positive cardiomyocytes (Figure 1F), the cross-sectional area of NRCMs (Supplemental Figure 4), the expression of fetal genes (ANP, BNP, β-MHC), and the level of the proliferation marker PCNA increased in time-dependent fashion (Figure 1G). The above results demonstrate AT1-AA exposure increased cardiomyocyte proliferation and size and prolonged the fetal phenotype, resulting in cardiac remodeling.

Exposure to AT1-AA induced differential microRNAs expression in fetal rat heart

The differentially expressed miRNAs in fetal rat hearts exposed to AT1-AA were detected by miRCURY™ LNA expression array. miRNAs with a fold change >2 were selected. The volcano plot identified upregulated and downregulated microRNAs (Supplemental Figure 5A). The heat map demonstrated 67 miRNAs differentially expressed in fetal hearts subjected to saline versus AT1-AA at gestation day 18 (Supplemental Figure 5B). 29 human-rat homologous (Figure 2A). The five most significantly altered candidate miRNAs were verified by qPCR *in vitro*. Consistent with the microRNA array *in vivo*, the up-regulation of miR-124-3p and the down-regulation of miR-181a-5p in AT1-AA-treated NRCMs were the most significant observed alterations (Figure 2B), and were consequently selected for follow up experiments. *In vivo* studies verified in utero AT1-AA exposure increased miR-124-3p and decreased miR-181a-5p expression in fetal hearts gestation day 18 (Figure 2C). Fluorescence in situ hybridization (FISH)

confirmed AT1-AA increased the expression of miR-124-3p and decreased the expression of miR-181a-5p in NRCMs. Both miRs were primarily distributed in the cytoplasm (Figures 2D, E).

The upregulation of miR-124-3p and downregulation of miR-181a-5p co-mediated AT1-AA induced cardiomyocytes overgrowth

miR-124-3p and miR-181a-5p were successfully overexpressed or inhibited in NRCMs (Supplemental Figure 6). Overexpression of miR-124-3p increased the expression of fetal genes (ANP, BNP, β-MHC), the cross-sectional area of cardiomyocytes, and the proportion of ki67-positive cardiomyocytes, while inhibition of miR-124-3p had the opposite effect (Figures 3A, C, Supplemental Figure 7A). In contrast, overexpression of miR-181a-5p suppressed the expression of fetal genes and decreased the cross-sectional area of cardiomyocytes and the proportion of ki67-positive cardiomyocytes, while miR-181a-5p inhibition had the opposite effect (Figures 3B, D, Supplemental Figure 7B). The above results suggest that miR-124-3p promoted cardiomyocytes overgrowth, while miR-181a-5p played a negative role.

Compared with the single transfection of a miR-124-3p mimic or miR-181a-5p inhibitor, the combined transfection of miR-124-3p mimic and miR-181a-5p inhibitor in NRCMs more potently increased fetal gene expression (Figure 3E), cardiomyocytes cross-sectional area (Supplemental Figure 8A), and proliferation (Figure 3G). We then evaluated whether miR-124-3p and miR-181a-5p co-regulated AT1-AA-induced cardiomyocytes' overgrowth. NRCMs were co-transfected with miR-124-3p mimic and miR-181a-5p inhibitor prior to AT1-AA exposure. Compared to AT1-AA stimulation alone, AT1-AA treatment after co-transfection of the miR-124-3p mimic and miR-181a-5p inhibitor significantly increased cardiac fetal gene expression (Figure 3F), cardiomyocyte cross-sectional area (Supplemental Figure 8B), and the proportion of ki67-positive cardiomyocytes (Figure 3H). These results indicated that the upregulation of miR-124-3p and downregulation of miR-181a-5p co-mediated AT1-AA induced cardiomyocyte overgrowth.

VCAN was the direct common target gene of miR-124-3p and miR-181a-5p

Prompted by the above results that miR-124-3p and miR-181a-5p jointly regulated AT1-AA-induced cardiac overgrowth, we next identified putative targets of miR-124-3p and miR-181a-5p. NRCMs were treated with PBS or AT1-AA for 24 hours. Proteins were isolated and analyzed by TMT^{TM} (tandem mass tags) labeled quantitative proteomics to screen differentially expressed genes (DEG). Genes with $P<0.05$ and fold change greater than 1.2 were selected (Supplemental Figure 9A). Potential target genes of *Homo sapiens* and *Rattus norvegicus* miR-124-3p and miR-181a-5p were predicted by TargetScan 7.2 and miRWalk 2.0 and intersected by *Venn Diagram Generator* (http://www.pangloss.com/seidel/Protocols/venn.cgi). These results were further intersected with the DEGs under AT1-AA exposure to obtain AT1-AA-related potential target genes (Figure 4A). Eight were associated with cardiac diseases (Figure 4B). In verifying the expression of AT1-AA-related potential target genes *in vivo* and *in vitro*, the expression of Versican (VCAN) increased most significantly (Supplemental Figure 9B, C).

During cardiac development, VCAN is a key regulator of cardiomyocyte proliferation. It is synthesized and secreted by cardiomyocytes and cardiac fibroblasts. *In vivo*, VCAN expression is increased in the hearts of E18 fetal rats AT1-AA treatment group compared to control (Figure 4C, E). *In vitro*, NRCMs treated with AT1-AA also exhibited greater VCAN expression (Figures 4D, F). miRWalk 2.0 identified miR-181a-5p bound to the 915-921 position of the 3'Untranslated region (UTR) of VCAN messenger RNA (mRNA), while miR-124-3p was bound to the 246-288 position of the 5'UTR of VCAN mRNA (Figures 4G, H). In order to verify the direct relationship of the two miRNAs and VCAN, vectors carrying the WT or MUTANT of 5'UTR or 3'UTR were constructed. HEK 293A cells were subjected a dual luciferase reporter gene assay. Cotransfection of miR-124-3p mimic and VCAN WT 5'UTR increased luciferase activity (Figure 4G); this effect was blocked by cotransfection of VCAN mutant 5'UTR. Conversely, cotransfection of miR-181a-5p mimic and VCAN WT 3'UTR decreased luciferase activity. This effect was blocked by contransfection of VCAN mutant 3'UTR (Figure 4H). These results confirmed VCAN as the common direct target gene of miR-124-3p and miR-181a-5p.

To clarify the role of miR-124-3p and miR-181a-5p on VCAN in cardiomyocytes, NRCMs were transfected with miR-124-3p/miR-181a-5p mimic, inhibitor, or negative control. Overexpression of miR-124-3p increased the expression of VCAN while inhibition of miR-124-3p decreased VCAN expression (Figure 4I). MiR-181a-5p mimic decreased VCAN expression, whereas miR-181a-5p inhibitor increased VCAN expression (Figure 4J).

To test whether miR-124-3p and miR-181a-5p influence VCAN expression, NRCMs were cotransfected with (1) miR-124-3p mimic and miR-181a inhibitor; (2) miR-124-3p inhibitor and miR-181a mimic; and then treated with AT1-AA or PBS for 24 hours. Cotransfection of miR-124-3p mimic and miR-181a-5p inhibitor significantly enhanced AT1-AA-induced increased VCAN expression (Figure 4K). Interestingly, when NRCMs were cotransfected with miR-124-3p inhibitor and miR-181a-5p mimic, VCAN expression was significantly decreased, and AT1-AA treatment had no effect (Figure 4L). These results suggest up-regulation of miR-124-3p and down-regulation of miR-181a-5p co-mediate increased VCAN expression induced by AT1-AA.

VCAN mediated AT1-AA-induced cardiomyocytes overgrowth and AT1-AA promoted extracellular VCAN secretion

We next determined the involvement of VCAN in AT1-AA induced cardiomyocytes overgrowth. Adenovirus vector carrying short hairpin RNA (shRNA) targeting VCAN was utilized to silence VCAN expression in NRCMs. NRCMs were then treated with AT1-AA or PBS for 24 hours. Silencing VCAN decreased fetal gene expression, cardiomyocyte cross-sectional area, the proportion of ki67-positive cardiomyocytes, and proliferation marker PCNA expression. Furthermore, in the setting of VCAN knockdown, AT1-AA administration did not influence the above outcomes (Figures 5A, B). These results suggest VCAN directly mediated AT1-AA induced cardiomyocytes overgrowth.

A secretory protein, VCAN is an influential component of the cardiac extracellular matrix, and a regulator of the extracellular space. To test whether AT1-AA prompted VCAN secretion, the culture supernatant of

NRCMs with or without AT1-AA treatment was collected. VCAN expression increased after AT1-AA treatment (Figure 5C, D). *In vivo*, VCAN levels in the serum of neonatal rats (postnatal day 0, P0, exposed to either saline control or AT1-AA in utero) was determined. Compared to control, AT1-AA exposure in utero increased VCAN secretion (Figure 5E). These results demonstrate AT1-AA promoted extracellular secretion of VCAN *in vivo* and *in vitro*. In the clinical setting, the umbilical cord blood of patients with preeclampsia exhibited increased AT1-AA P/N (Figure 5F) and VCAN expression (Figure 5G) compared to normal healthy patients. Pearson correlation analysis confirmed that VCAN expression in umbilical cord blood of preeclamptc patients was positively correlated with the P/N value of AT1-AA (Figure 5H). In concert, the basic science and clinical results of this experiment together suggest VCAN may serve as a biomarker reflecting AT1-AA-induced cardiac injury in utero and post-birth.

Discussion

Our previous study on rodents demonstrated AT1-AA exposure in utero resulted in cardiac dysfunction and altered cardiac structure in the early life of offspring[21]. In this study, we demonstrate AT1-AA up-regulated miR-124-3p and down-regulated miR-181a-5p. Dysregulation of these two miRNAs together promotes VCAN expression. Increased VCAN expression induced cardiomyocyte overgrowth, ultimately causing cardiac remodeling. Whereas miR-181a-5p binds the 3'UTR of VCAN mRNA (inhibiting its protein expression), miR-124-3p binds the 5'UTR of VCAN mRNA (promoting VCAN expression). VCAN was up-regulated in the serum of the neonatal offspring of AT1-AA-positive pregnant rats, as well as the umbilical cord blood of AT1-AA-positive preeclampsia patients.

Accumulating evidence demonstrates that AT1-AA is harmful to preeclamptic patients. However, its effect upon offspring, and any underlying responsible mechanisms, are not clear. In this study, AT1-AA exposure induced cardiac remodeling, evidenced by increased cardiomyocyte proliferation, cross-sectional area, and fetal gene expression. Proliferation is necessary for heart development, but excessive proliferation is deleterious for fetuses. Hypertrophy or hyperplasia increase cardiac mass and cardiac hyperplasia predominates during mammalian fetal life[24]. For example, high salt exposure increases cardiomyocyte proliferation, apoptosis, and delays differentiation, thereby increasing embryonic mortality[25]. High glucose exposure results in fetal cardiac hyperplasia[26]. Fetal genes such as ANP, BNP, and β-MHC are highly expressed in the early developing stages of the fetal heart, and are downregulated after birth. During pathologic cardiac remodeling, fetal genes are reactivated[27,28]. In our study, fetal genes increase after AT1-AA exposure *in vivo* and *in vitro*, indicating that immature cardiomyocytes maladaptively responded to pressure overload by hypertrophic growth and overproliferation.

To clarify whether AT1-AA directly promoted cardiomyocyte enlargement and proliferation via AT1R, AT1R knockout neonatal rat cardiomyocytes (Supplemental Fig. 10A) were used. No significant change of fetal genes was observed after AT1-AA administration (Supplemental Fig. 10B). Moreover, AT1R-ECII peptide completely neutralized the adverse effects of AT1-AA exposure (Supplemental Fig. 10D), suggesting AT1 receptor-dependent AT1-AA activity. Unexpectedly, telmisartan (TST), a recognized AT1R blocker, only

partially blocked the pro-remodeling effect of AT1-AA *in vitro* (Supplemental Fig. 10C), suggesting AT1-AA activates AT1R in a non-classical manner.

AT1-AA is an immunoglobulin of the IgG class[29]. To elucidate whether the pro-remodeling effect is a common effect of total IgG or a unique effect of AT1-AA, we observed the effect of AT1-AA-negative IgG (IgG without ability to increase beating frequency of NRCMs) exposure *in vivo* and *in vitro*. No significant changes were found between control and IgG group (Supplemental Fig. 11A-D, Supplemental Fig. 12B), indicating AT1-AA mediated cardiomyocyte proliferation and enlargement effects were unique. For this reason, only the AT1-AA group and saline control groups persisted in subsequent experiments.

Angiotensin II (Ang II) is the natural ligand of AT1R. To further confirm the relationship between AT1R activation and fetal cardiac remodeling, pregnant rats were continuously infused with Ang II from E13 to E18 by micropump. Similar to AT1-AA, at gestation day 18, fetal rats in the Ang II group exhibited increased HW/BW ratio (Supplemental Fig. 11A), a thickened left ventricular wall and increased cardiomyocyte area (Supplemental Fig. 11B), a greater proportion of ki67-positive cardiomyocytes (Supplemental Fig. 11C), and increased expression of fetal genes and proliferation marker PCNA (Supplemental Fig. 11D). *In vitro*, Ang II had the same effect on NRCMs (Supplemental Fig. 12A). These results indicate that intrauterine AT1R overactivation contributed to pathologic cardiac remodeling at an early stage of life. Of note, circulating Ang II levels were significantly decreased in preeclamptic patients compared to healthy, normal pregnant women[30]. We will no longer focus upon mechanisms involving Ang II in follow-up investigations.

MicroRNAs regulate cardiac gene expression, but also influence cardiac development and various pathologic processes [31]. Classically, microRNAs induce mRNA degradation or inhibit translation by binding to the 3’UTR of target gene mRNAs, thereby having post-transcriptional influence. Emerging evidence demonstrates microRNAs also upregulate target gene expression by binding to the 5’UTR of target gene mRNA [31], suggesting the 3’UTR is not the only binding site of the microRNA. In our study, markedly increased miR-124-3p and decreased miR-181a-5p were observed concomitantly in the fetal heart of the AT1-AA group. Recently, several studies have demonstrated the importance of miR-124-3p and miR-181a-5p in cardiac disease. miR-124-3p induced cardiomyocyte apoptosis in myocardial infarction [34], whereas miR-181a-5p inhibited cardiomyocyte apoptosis [35] and reduced myocardial ischemia-reperfusion injury[36]. Here, we demonstrate that increased miR-124-3p and decreased miR-181a-5p in concert promoted fetal cardiac remodeling after AT1-AA exposure. We demonstrate that VCAN was the common target gene of miR-181a-5p and miR-124-3p. The binding of upregulated miR-124-3p to the 5’UTR of VCAN mRNA promoted VCAN expression, while the downregulation of miR-181a-5p (bound to the 3’UTR of VCAN mRNA) mitigated VCAN inhibition.

A member of the chondroitin sulfate proteoglycan family, VCAN is necessary for cardiac development[37]. VCAN is produced by both cardiomyocytes and cardiac fibroblasts[38]. During mouse heart development, VCAN expression exhibits strong spatiotemporal specificity. In early development, the heart grows through cardiomyocyte replication. High VCAN expression is accompanied by the rapid proliferation of

cardiomyocytes, ensuring normal heart development. Cardiac VCAN expression reaches peak at gestation day 13.5. At the completion of development, VCAN is hydrolyzed to inhibit cardiomyocyte proliferation, prompting the switch of cardiac development mode[39,40]. After birth, cardiac VCAN expression is minimal. In our study, AT1-AA exposure increased fetal heart VCAN expression on gestation day 18, accompanied by increased cardiomyocyte proliferation. Sustained cardiomyocyte proliferation may result in fatal congestive heart failure before or after birth[41,42]. Therefore, inappropriate VCAN reactivation adversely affects the heart.

VCAN is secreted when cells proliferate or migrate[43,44]. During pathologic atherosclerosis, secreted VCAN regulates lipoprotein expression[45]. Based on these prior studies, we detected extracellular VCAN expression. We chose neonatal rats to collect serum, because it was difficult to collect fetal blood on gestation day 18, and the hypertrophic effect of AT1-AA persisted until postnatal birth (Supplemental Fig. 13). Pertaining to clinical samples, umbilical cord blood (UCB) was collected after delivery and umbilical cord ligation, because UCB biomarkers may reflect fetal heart development[46]. Compared to healthy pregnant women, PE patients exhibited increased VCAN UCB expression. In 2007, Tomasz Gogiel et al. reported an increase in VCAN expression in the umbilical vein wall of preeclamptic pregnant women [47], suggesting AT1-AA may importantly influence increased VCAN expression. However, whether serum VCAN may serve as an early biomarker reflecting cardiac injury in offspring requires additional clinical study confirmation.

The DOHaD theory suggests that appropriate intervention in early life is important for the prevention and treatment of CVD in adulthood. Presently, the treatment of preeclampsia remains a worldwide problem. Symptomatic treatement of the mother remains the mainstay of preventing injury to offspring. Most preeclamptic patients manifest high serum AT1-AA titers[11]. Our findings further suggest that offspring exposed to AT1-AA during pregnancy undergo cardiac remodeling in utero. Although some studies have shown that AT1-AA can be blocked by AT1R blockers, AT1R blockers have teratogenic effects on the fetuses [48,49]. Therefore, it is of great clinical significance to discover novel, safe treatment strategies. In the past decade, many studies have confirmed that differentially expressed microRNAs are a key feature of preeclampsia [48,49]. Our current study identifies miR-124-3p and miR-181a-5p co-participate in AT1-AA-induced fetal cardiac remodeling. Targeting these microRNA may potentially prevent early cardiac injury in the offspring of preeclamptic patients.

Abbreviations

Cardiovascular disease (CVD)

Autoantibodies against angiotensin II type 1 receptor (AT1-AA)

Neonatal rat cardiomyocytes (NRCMs)

Untranslated Region (UTR)

Angiotensin II- type 1 receptor (AT1R)

The extracellular second loop of AT1R (AT1R-ECII)

Developmental Origins of Health and Disease (DoHAD)

Preeclampsia (PE)

Renin-angiotensin system (RAS)

Versican (VCAN)

Telmisartan (TST)

Declarations

Acknowledgments

We sincerely thank Baodi Hospital for assistance in subject blood sample collection.

Competing interests

None

Funding Statement

This work was supported by the National Natural Science Foundation of China (No. 31771267, 81800425) and the Open Fund from the Key Laboratory of Cellular Physiology (Shanxi Medical University), Ministry of Education, China (KLMEC/SXMU-201902).

References

1. Barker, D.J., In utero programming of chronic disease. *Clin Sci (Lond)* **95** 115: (1998)
2. Langley-Evans, S.C., McMullen, S., Developmental origins of adult disease. *Med Princ Pract* **19** 87: (2010)
3. Crispi, F., et al., Main Patterns of Fetal Cardiac Remodeling. *FETAL DIAGN THER* **47** 337: (2020)
4. Palinski, W., Effect of maternal cardiovascular conditions and risk factors on offspring cardiovascular disease. *CIRCULATION* **129** 2066: (2014)
5. Fraser, A., Nelson, S.M., Macdonald-Wallis, C., Sattar, N., Lawlor, D.A., Hypertensive disorders of pregnancy and cardiometabolic health in adolescent offspring. *HYPERTENSION* **62** 614: (2013)
6. Fox, R., Kitt, J., Leeson, P., Aye, C., Lewandowski, A.J., Preeclampsia: Risk Factors, Diagnosis, Management, and the Cardiovascular Impact on the Offspring. *J CLIN MED* **8**: (2019)

7. Herrera-Garcia, G., Contag, S., Maternal preeclampsia and risk for cardiovascular disease in offspring. *CURR HYPERTENS REP* **16** 475: (2014)
8. Nahum, S.K., et al., Prenatal exposure to preeclampsia as an independent risk factor for long-term cardiovascular morbidity of the offspring. *PREGNANCY HYPERTENS* **13** 181: (2018)
9. Steinberger, J., Preeclampsia and cardiovascular risk in offspring. *J Pediatr* **208** 1: (2019)
10. Irani, R.A., Xia, Y., Renin angiotensin signaling in normal pregnancy and preeclampsia. *SEMIN NEPHROL* **31** 47: (2011)
11. Wallukat, G., et al., Patients with preeclampsia develop agonistic autoantibodies against the angiotensin AT1 receptor. *J CLIN INVEST* **103** 945: (1999)
12. Chai, W., et al., Angiotensin II type I receptor agonistic autoantibody-induced apoptosis in neonatal rat cardiomyocytes is dependent on the generation of tumor necrosis factor-alpha. *Acta Biochim Biophys Sin (Shanghai)* **44** 984: (2012)
13. Zhang, S., et al., Angiotensin type 1 receptor autoantibody from preeclamptic patients induces human fetoplacental vasoconstriction. *J CELL PHYSIOL* **228** 142: (2013)
14. Zhou, C.C., et al., Angiotensin receptor agonistic autoantibody-mediated tumor necrosis factor-alpha induction contributes to increased soluble endoglin production in preeclampsia. *CIRCULATION* **121** 436: (2010)
15. Xia, Y., Wen, H., Bobst, S., Day, M.C., Kellems, R.E., Maternal autoantibodies from preeclamptic patients activate angiotensin receptors on human trophoblast cells. *J Soc Gynecol Investig* **10** 82: (2003)
16. Zhang, S., et al., Increased susceptibility to metabolic syndrome in adult offspring of angiotensin type 1 receptor autoantibody-positive rats. *Antioxid Redox Signal* **17** 733: (2012)
17. Bai, L., et al., AT1-receptor autoantibody exposure in utero contributes to cardiac dysfunction and increased glycolysis in fetal mice. *Acta Biochim Biophys Sin (Shanghai)* **52** 1373: (2020)
18. van Rooij, E., The art of microRNA research. *CIRC RES* **108** 219: (2011)
19. Bernardo, B.C., Ooi, J.Y., Lin, R.C., McMullen, J.R., miRNA therapeutics: a new class of drugs with potential therapeutic applications in the heart. *FUTURE MED CHEM* **7** 1771: (2015)
20. ACOG Practice Bulletin No: 202: Gestational Hypertension and Preeclampsia. OBSTET. GYNECOL. **133**, 1 (2019)
21. Bai, L., et al., AT1-receptor autoantibody exposure in utero contributes to cardiac dysfunction and increased glycolysis in fetal mice. *Acta Biochim Biophys Sin (Shanghai)* **52** 1373: (2020)
22. Zhang, S., et al., Hyperinsulinemia precedes insulin resistance in offspring rats exposed to angiotensin II type 1 autoantibody in utero. *ENDOCRINE* **62** 588: (2018)
23. Wei, M., et al., Preparation and Biological Activity of the Monoclonal Antibody against the Second Extracellular Loop of the Angiotensin II Type 1 Receptor. *J IMMUNOL RES* 2016 1858252 (2016)
24. Oparil, S., Bishop, S.P., Clubb, F.J., Myocardial cell hypertrophy or hyperplasia. *HYPERTENSION* **6** I38: (1984)

25. Wang, G., et al., The impact of high-salt exposure on cardiovascular development in the early chick embryo. *J EXP BIOL* **218** 3468: (2015)
26. Jin, Y.M., et al., High glucose level induces cardiovascular dysplasia during early embryo development. *Exp Clin Endocrinol Diabetes* **121** 448: (2013)
27. Man, J., Barnett, P., Christoffels, V.M., Structure and function of the Nppa-Nppb cluster locus during heart development and disease. *CELL MOL LIFE SCI* **75** 1435: (2018)
28. Kuwahara, K., Nishikimi, T., Nakao, K., Transcriptional regulation of the fetal cardiac gene program. *J PHARMACOL SCI* **119** 198: (2012)
29. Wallukat, G., et al., Patients with preeclampsia develop agonistic autoantibodies against the angiotensin AT1 receptor. *J CLIN INVEST* **103** 945: (1999)
30. Irani, R.A., Xia, Y., The functional role of the renin-angiotensin system in pregnancy and preeclampsia. *PLACENTA* **29** 763: (2008)
31. Small, E.M., Olson, E.N., Pervasive roles of microRNAs in cardiovascular biology. *NATURE* **469** 336: (2011)
32. Orom, U.A., Nielsen, F.C., Lund, A.H., MicroRNA-10a binds the 5'UTR of ribosomal protein mRNAs and enhances their translation. *MOL CELL* **30** 460: (2008)
33. Li, H., et al., Nuclear miR-320 Mediates Diabetes-Induced Cardiac Dysfunction by Activating Transcription of Fatty Acid Metabolic Genes to Cause Lipotoxicity in the Heart. *CIRC RES* **125** 1106: (2019)
34. Liu, B.F., Chen, Q., Zhang, M., Zhu, Y.K., MiR-124 promotes ischemia-reperfusion induced cardiomyocyte apoptosis by targeting sphingosine kinase 1. *Eur Rev Med Pharmacol Sci* **23** 7049: (2019)
35. Zhu, J., et al., miR-181a and miR-150 regulate dendritic cell immune inflammatory responses and cardiomyocyte apoptosis via targeting JAK1-STAT1/c-Fos pathway. *J CELL MOL MED* **21** 2884: (2017)
36. Zhang, L.X., et al., MiR-181a affects myocardial ischemia-reperfusion injury in rats via regulating akt signaling pathway. *Eur Rev Med Pharmacol Sci* **23** 6292: (2019)
37. Burns, T.A., et al., Imbalanced expression of Vcan mRNA splice form proteins alters heart morphology and cellular protein profiles. *PLOS ONE* **9** e89133: (2014)
38. Chan, C.K., et al., Differentiation of cardiomyocytes from human embryonic stem cells is accompanied by changes in the extracellular matrix production of versican and hyaluronan. *J CELL BIOCHEM* **111** 585: (2010)
39. Cooley, M.A., et al., Fibulin-1 is required during cardiac ventricular morphogenesis for versican cleavage, suppression of ErbB2 and Erk1/2 activation, and to attenuate trabecular cardiomyocyte proliferation. *Dev Dyn* **241** 303: (2012)
40. Silva, A.C., Pereira, C., Fonseca, A., Pinto-do-O, P., Nascimento, D.S.: Bearing My Heart: The Role of Extracellular Matrix on Cardiac Development, Homeostasis, and Injury Response. Front. Cell. Dev.

Biol. **8**, 621644 (2020)

41. Nolan, C.M., Lawlor, M.A., Variable accumulation of insulin-like growth factor II in mouse tissues deficient in insulin-like growth factor II receptor. *Int J Biochem Cell Biol* **31** 1421: (1999)
42. Lau, M.M., et al.: Loss of the imprinted IGF2/cation-independent mannose 6-phosphate receptor results in fetal overgrowth and perinatal lethality. Genes Dev. **8**, 2953 (1994)
43. Evanko, S.P., Tammi, M.I., Tammi, R.H., Wight, T.N., Hyaluronan-dependent pericellular matrix. *Adv Drug Deliv Rev* **59** 1351: (2007)
44. Evanko, S.P., Angello, J.C., Wight, T.N., Formation of hyaluronan- and versican-rich pericellular matrix is required for proliferation and migration of vascular smooth muscle cells. *Arterioscler Thromb Vasc Biol* **19** 1004: (1999)
45. Asplund, A., et al., Hypoxic regulation of secreted proteoglycans in macrophages. *GLYCOBIOLOGY* **20** 33: (2010)
46. Perez-Cruz, M., et al., Cord Blood Biomarkers of Cardiac Dysfunction and Damage in Term Growth-Restricted Fetuses Classified by Severity Criteria. *FETAL DIAGN THER* **44** 271: (2018)
47. Gogiel, T., Galewska, Z., Romanowicz, L., Jaworski, S., Bankowski, E., Pre-eclampsia-associated alterations in decorin, biglycan and versican of the umbilical cord vein wall. *Eur J Obstet Gynecol Reprod Biol* **134** 51: (2007)
48. Korkes, H.A., et al., Human fetal malformations associated with the use of an angiotensin II receptor antagonist: case report. *J Bras Nefrol* **36** 410: (2014)
49. Sanchez, S.I., Seltzer, A.M., Fuentes, L.B., Forneris, M.L., Ciuffo, G.M., Inhibition of Angiotensin II receptors during pregnancy induces malformations in developing rat kidney. *EUR J PHARMACOL* **588** 114: (2008)
50. Skalis, G., et al., MicroRNAs in Preeclampsia. *Microrna* **8** 28: (2019)

Figures

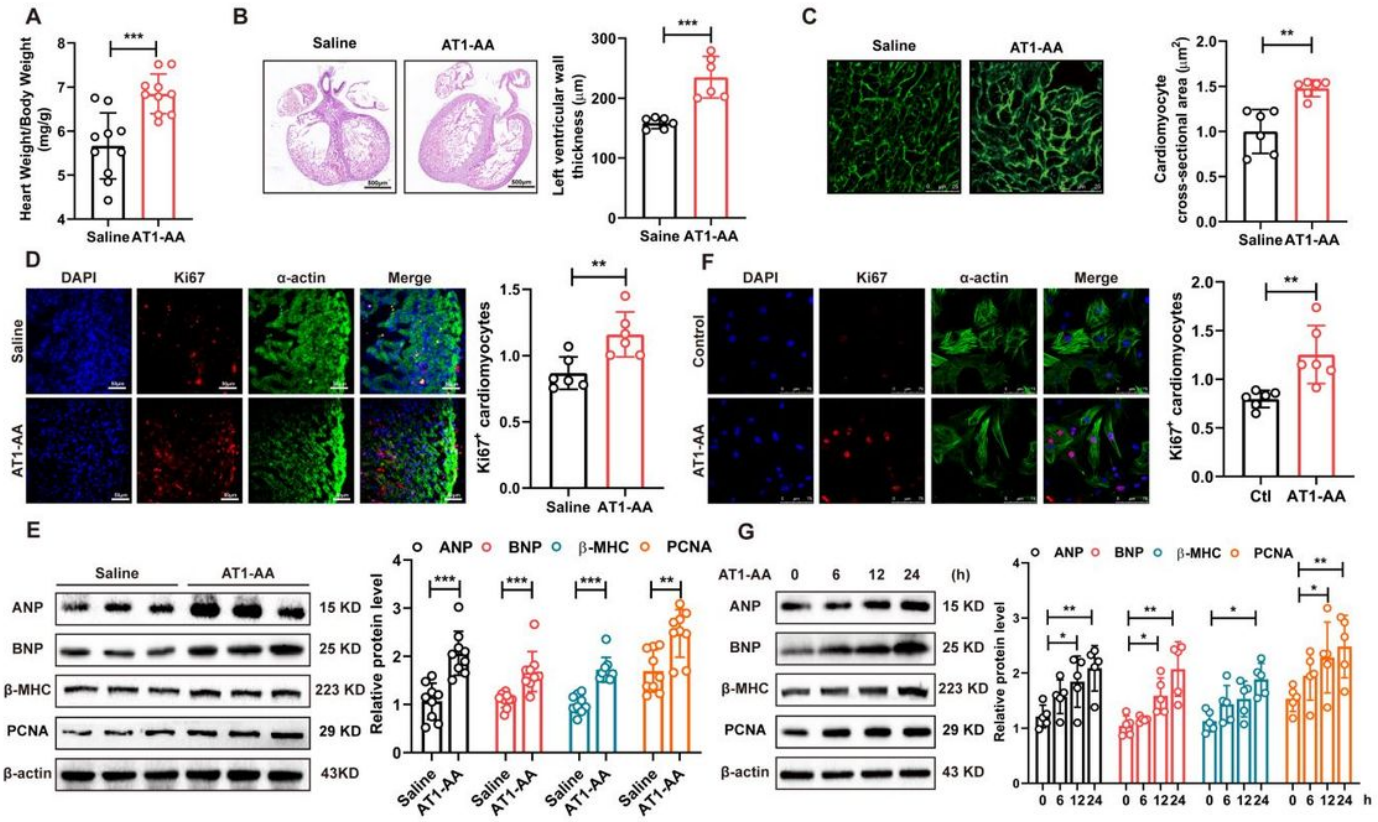

Figure 1

AT1-AA induced cardiomyocyte proliferation and enlargement *in vivo* and *in vitro*.

(A) Heart weight/body weight (HW/BW) ratio of fetal rat hearts on gestation day 18 (n=10). (B) H&E staining of fetal hearts (Bars=200 μm, n=6). (C) Wheat germ agglutinin (WGA) staining of left ventricular section (Bars=25 μm, n=6). (D) Immunofluorescence (IF) staining of left ventricular section (n=8). Bars=50 μm. (E) Expression of ANP, BNP, β-MHC, and PCNA of E18 fetal hearts measured by Western blot (n=8). (F) IF staining of ki67 and α-actin of neonatal rat cardiomyocytes (NRCM). Nuclei stained with DAPI (n=6-9 per group). Bars=75 μm. (G) Expression of ANP, BNP, β-MHC, and PCNA of NRCM measured by Western blot (n=5). Independent sample t-test and one-way ANOVA used for statistical analysis. *p<0.05, **p<0.01, and ***p<0.001.

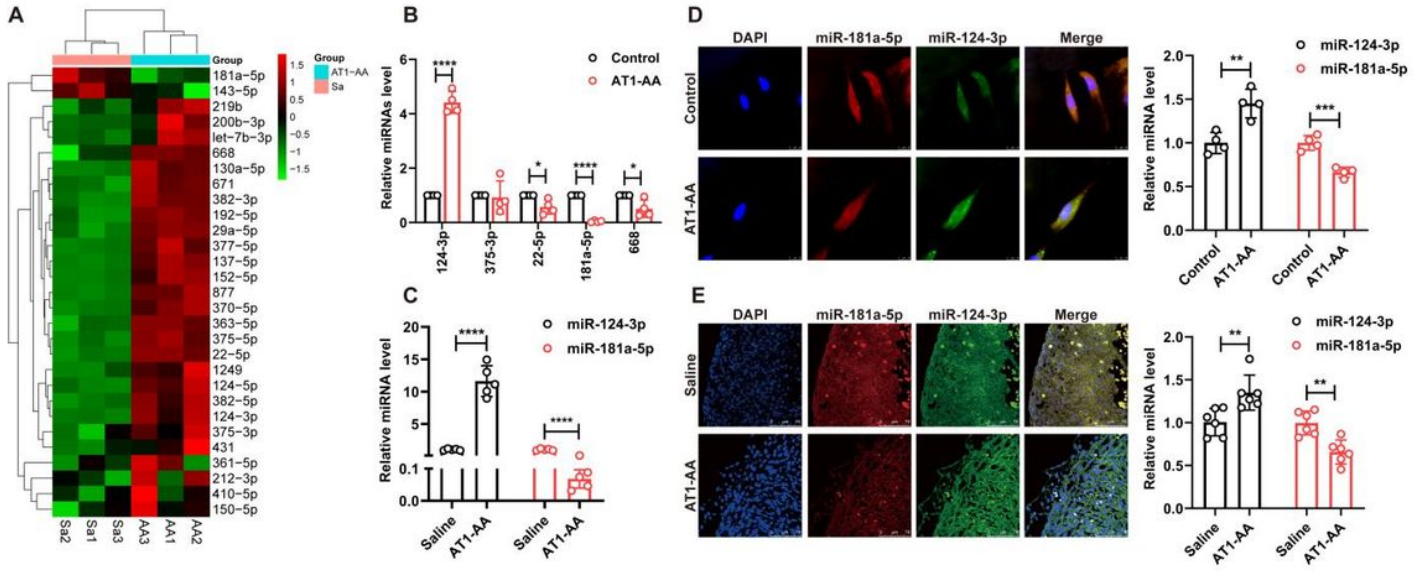

Figure 2

AT1-AA induced microRNAs changes in the fetal rat heart.

(A) Heat map of homologous differentially expressed microRNAs in the fetal rat versus human heart, on E18 (Fold change>2.0, n=5-6 per group). (B) Verification of 5 distinctly altered microRNAs in NRCMs was measured by qPCR (n=4). (C) Expression of miR-124-3p and miR-181a-5p in fetal rat hearts was verified by qPCR (n=4). (D) Representative expression and localization of miR-124-3p and miR-181a-5p in NRCMs evidenced by fluorescence in situ hybridization (FISH, n=4). Bars=10 μm. (E) miR-124-3p and miR-181a-5p in fetal rat hearts at gestation day 18 exhibited by FISH (Bars=75 μm, n=8). Independent sample t-test and one-way ANOVA used for statistical analysis. *p<0.05, **p<0.01, ***p<0.001, and ****p<0.0001.

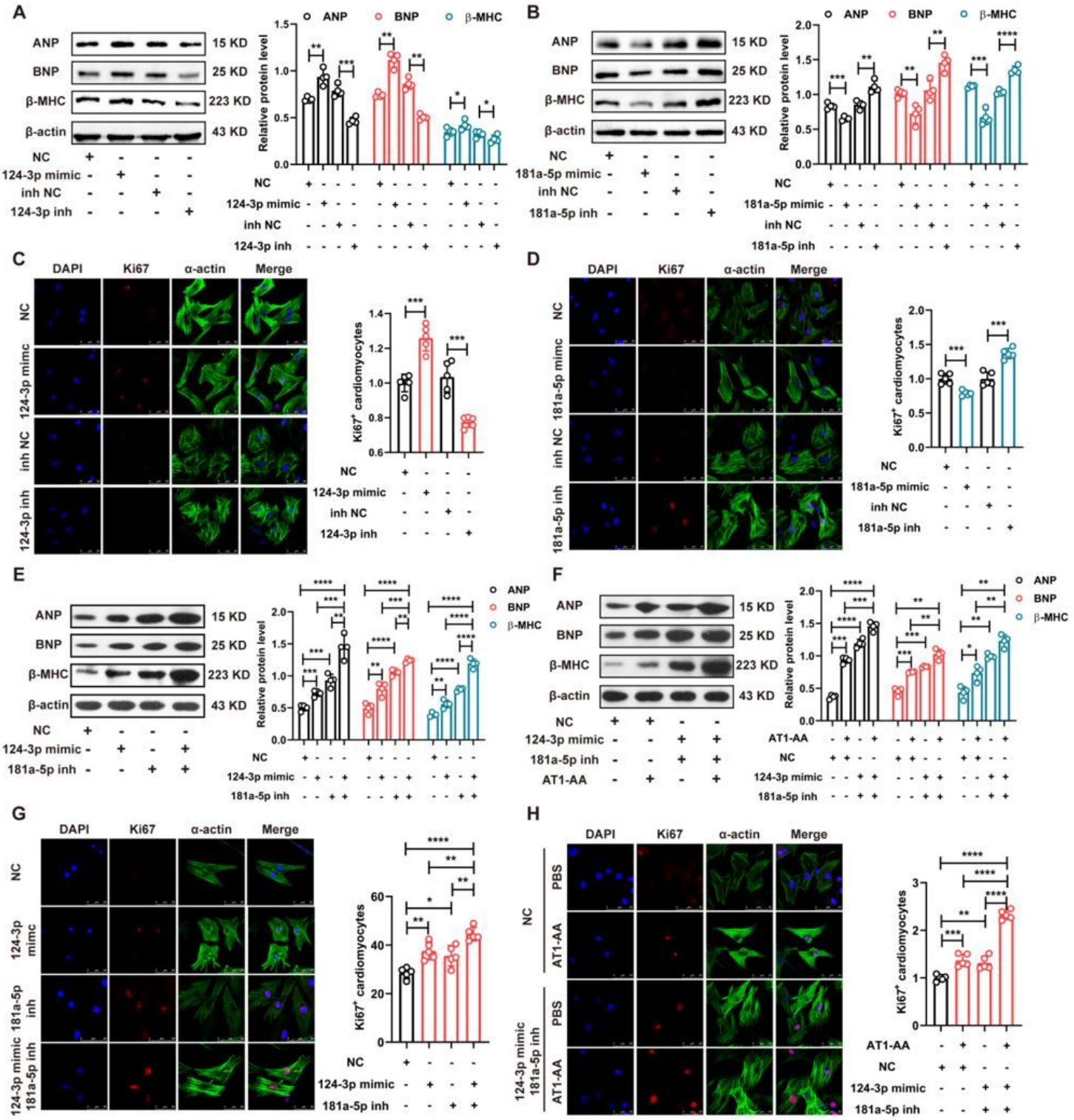

Figure 3

Increased miR-124-3p in combination with decreased miR-181a-5p promotes cardiomyocyte proliferation and enlargement induced by AT1-AA.

(A) Fetal genes were detected in NRCMs by Western blot after overexpressing or inhibiting miR-124-3p (n=4). *p<0.05, **p<0.01, and ***p<0.001 compared to NC or inh NC. (B) NRCMs were transfected with

miR-181a-5p mimic and inhibitor, and fetal genes were detected by Western blot (n=4). (C) IF staining of α-actin and ki67 were measured in NRCMs after overexpression or inhibition of miR-124-3p (n=5). Nuclei were stained with DAPI. Bars=50 μm. (D) IF staining of α-actin and ki67 was performed in NRCMs after transfection of miR-181a-5p mimic or inhibitor (n=5). Nuclei were stained with DAPI. Bars=50 μm. NRCMs were transfected with miR-124-3p mimic, miR-181a-5p inhibitor, or both. Fetal genes were detected by Western blot (n=4). (F) NRCMs were co-transfected with miR-124-3p mimic and miR-181a-5p inhibitor with or without AT1-AA. Fetal genes were detected by Western blot (n=4). (G) After transfection of the indicated RNA (miR-124-3p mimic, miR-181a-5p inhibitor), IF staining of α-actin and ki67 was performed (n=5). Nuclei were stained with DAPI. Bars=50 μm. (H) α-actin and ki67 staining were measured in NRCM after combination overexpression of miR-124-3p and inhibition of miR-181a-5p, with or without AT1-AA (n=5). Nuclei was stained with DAPI. Bars=50 μm. Independent sample t-test and one-way ANOVA were used for statistical analysis. *$p<0.05$, **$p<0.01$, ***$p<0.001$, and ****$p<0.0001$.

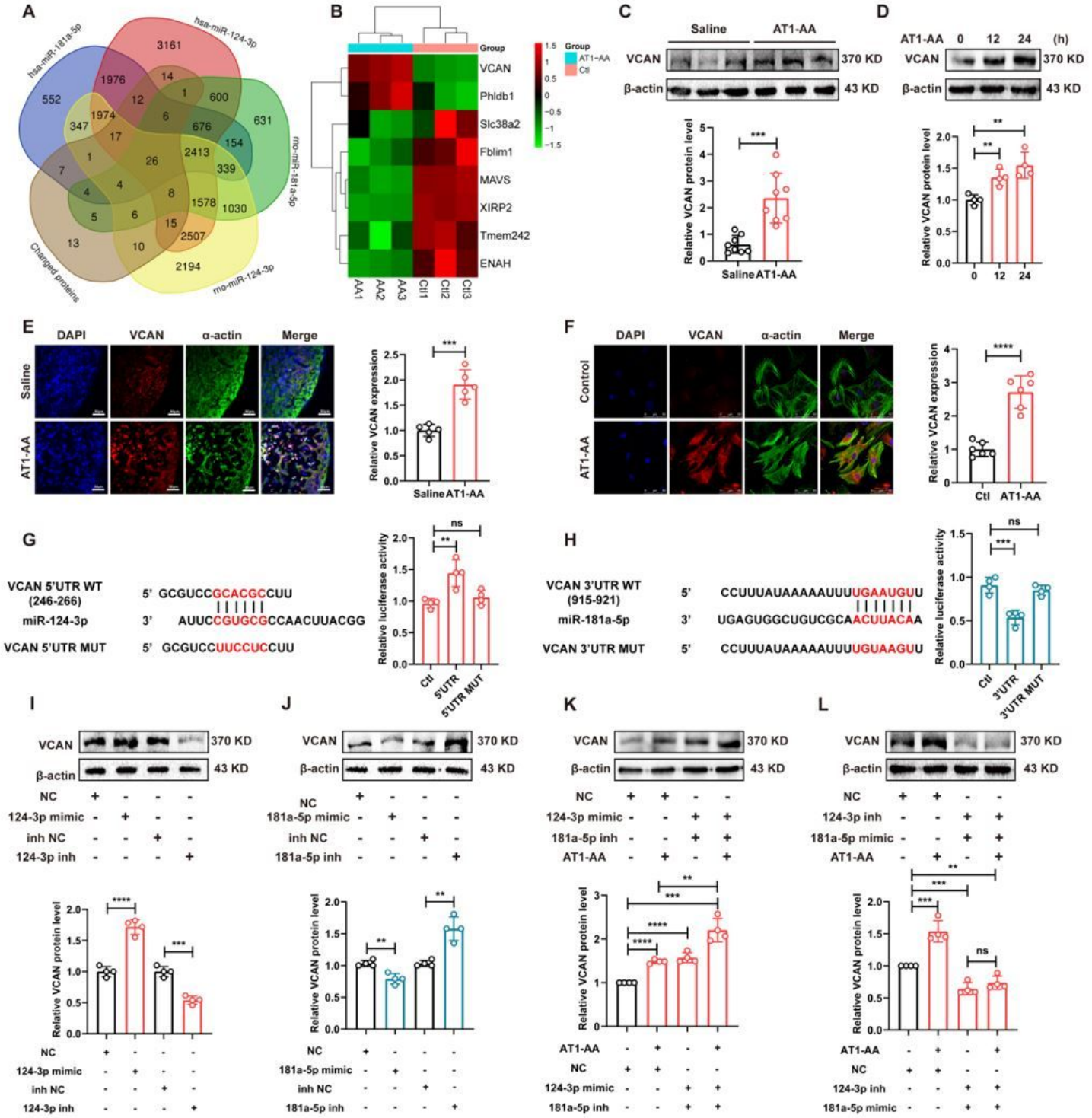

Figure 4

VCAN was the direct target gene of miR-124-3p and miR-181a-5p.

(A) Diagram of the intersection of common potential target genes of has-miR-124-3hashsa-miR-181a-5p, rno-miR-124-3p, and rno-miR-181a-5p. (B) Heat map of potential target genes differentially expressed in NRCMs after AT1-AA stimulation also related to cardiac diseases. (C) VCAN expression verified by Western blot in E18 fetal rat hearts. (n=8). (D) Western blot demonstrating VCAN expression after AT1-AA

treatment in NRCMs (0, 12, and 24 hours, n=4). (E) VCAN expression and distribution *in vivo* was measured by IF staining (n=6). Bars=50 μm. (F) IF staining indicating expression and localization of VCAN in NRCMs (n=6). Bars=50 μm. (G) Prediction of binding sites of miR-124-3p with 5'UTR of VCAN mRNA. HEK 293A cell co-transfected with psicheck2-VCAN-5'UTR and miR-124-3p mimic or negative control (NC) was measured by luciferase reporter gene analysis to detect luciferase activity (n=4). (H) Prediction of binding sites of miR-181a-5p with 3'UTR of VCAN mRNA. HEK 293A cell co-transfected with psicheck2-VCAN-3'UTR and miR-181a-5p mimic or NC was measured by luciferase reporter gene analysis (n=4). (I) Expression of VCAN *in vitro* was detected by Western blot after transfection with miR-124-3p mimic or inhibitor (n=4). (J) Transfection of miR-181a-5p mimic or inhibitor was performed in NRCMs. VCAN protein level detected by Western blot (n=4). (K) NRCMs were co-transfected with miR-124-3p mimic and miR-181a-5p inhibitor with or without AT1-AA . VCAN expression was measured by Western blot (n=4). (L) After co-transfection of miR-124-3p inhibitor and miR-181a-5p mimic with or without AT1-AA, VCAN expression was measured by Western blot (n=4). Independent sample t-test and one-way ANOVA were used for statistical analysis. **$p<0.01$, ***$p<0.001$, and ****$p<0.0001$. ns=no significant changes.

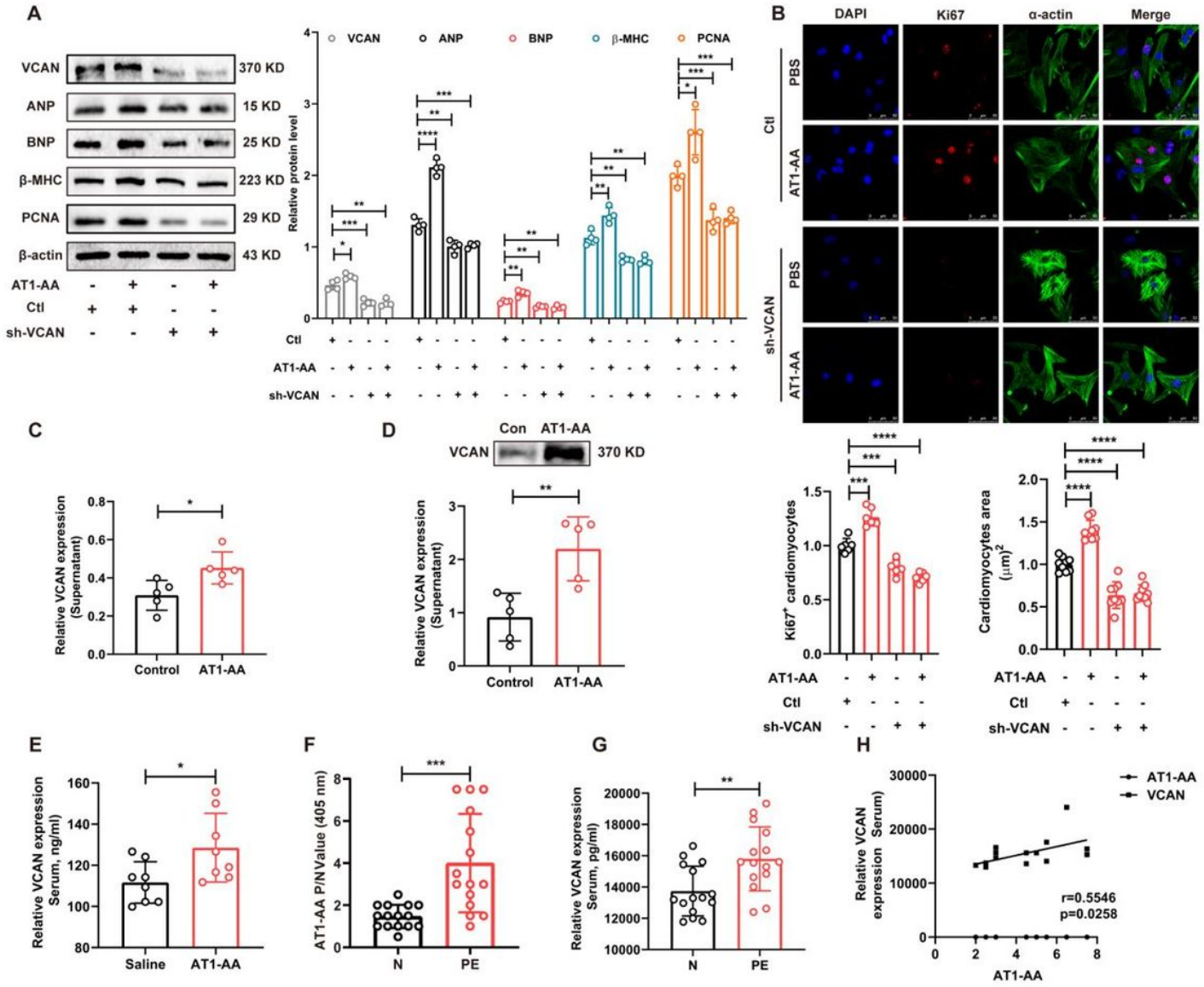

Figure 5

AT1-AA induced enlargement and proliferation of cardiomyocytes by promoting both VCAN expression and secretion.

(A) After successful knockdown of VCAN, NRCM was treated with or without AT1-AA. Relative expression of VCAN, fetal genes, and PCNA were detected by Western blot (n=4). (B) Ki67 staining was performed after VCAN knockdown and AT1-AA exposure (n=6). Bar=50 μm. (C) VCAN expression in supernatant of NRCMs with or without AT1-AA stimulation was measured by ELISA (n=5). (D) VCAN expression in supernatant of NRCMs was detected by Western blot after AT1-AA treatment (n=5). (E) Serum VCAN expression in neonatal (postnatal day 0) rat hearts was detected by ELISA (n=8). (F) AT1-AA and (G) VCAN expression in umbilical cord blood from normal pregnancy (N) and preeclamptic patients (PE) was measured by ELISA (n=15). (H) Pearson correlation analysis between AT1-AA OD value and VCAN expression in patients with preeclampsia (n=15, r=0.5546, p=0.0258). Independent sample t-test, one-way

ANOVA and Pearson test were used for statistical analysis. *$p<0.05$, **$p<0.01$, ***$p<0.001$, and ****$p<0.0001$.

Supplementary Files

This is a list of supplementary files associated with this preprint. Click to download.

- SupplementaryMaterial.docx